

Router Node Placement With Service Priority in Wireless Mesh Networks Using Simulated Annealing With Momentum Terms

Chun-Cheng Lin, *Member, IEEE*, Lei Shu, *Member, IEEE*, and Der-Jiunn Deng, *Member, IEEE*

Abstract—In wireless mesh networks (WMNs), mesh clients communicate with each other via the gateway and bridging functions of mesh routers. The performance of a WMN is generally affected by its network connectivity and client coverage, both of which are determined by its router node placement (RNP) in the deployment area. For simplicity, previous works considered only the RNP where each mesh client is served as an equal. In practice, however, mesh clients should be served with different priorities owing to factors such as their importance and their different payments for the service access. To fulfil this requirement, by assuming that each mesh client is also associated with a service priority, this paper investigates an RNP problem with a service priority constraint in which the mesh clients with service priorities higher than a threshold must be served. Given that this problem inherited from the complexity of the original RNP problem is computationally intractable in general, this paper also develops a novel simulated annealing (SA) approach that takes into account momentum terms to improve the efficiency and accuracy of annealing schedules and prevent fluctuations in values of the acceptance probability function. Additionally, the time complexity of the proposed SA algorithm is analyzed. Furthermore, evaluation of different-size instances under various parameters and annealing schedules demonstrates the superiority of the proposed approach.

Index Terms—Annealing schedule, router node placement (RNP), simulated annealing (SA), wireless mesh network (WMN).

I. INTRODUCTION

ADVANCES in multiradio and multichannel technologies have led to the emergence of wireless mesh networks (WMNs), which are capable of offering high-speed Internet access for mobile users without time or location constraints and achieving a greater cost-efficient design and deployment than

those of conventional networks based on wired connections. A detailed survey on WMNs can be found in [1]. Owing to the generally complex nature of problems associated with each layer of WMNs, most studies have focused on the simplified problems after some degree of abstraction and assumptions. To fulfill more practical requirements, WMNs face various challenges, including link scheduling [2], gateway selection [3], routing problems with different concerns [4], and assignment problems for multichannel WMNs [5]–[7].

WMNs are composed of mesh clients and mesh routers, in which mesh routers serve as the access points that allow mesh clients to access the Internet and to connect to other mesh routers through point-to-point wireless communication. Router node placement in WMNs (WMN-RNP for short) involves placing mesh routes in a geographical deployment area in order to optimize some performance measures of WMNs. The previous works for the WMN-RNP problem can generally be classified into two categories. The first category focuses on tailoring the problem model by adding different objectives and mesh nodes for fulfilling practical requirements, including throughput optimization for gateway placement [4], [9], biobjective RNP for two-tier WMNs [10], and multiobjective WMN-RNP [11]. Exact optimal solutions for the WMN-RNP problem are generally unattainable in deterministic polynomial time. Therefore, the second category of previous works focuses on designing metaheuristic approaches, including local search algorithm [12], simulated annealing (SA) [13], genetic algorithm [14], tabu search [15], and particle swarm optimization [16].

To our knowledge, the previous works on the WMN-RNP problem assume that all mesh clients are treated as an equal when evaluating network performance. In practice, however, WMNs may differ in performance (e.g., network connectivity, stability, and quality of service) owing to factors such as the increasing demand for service, interference from other wireless devices, and surrounding environments. Therefore, some of the mesh clients may be willing to pay more for higher quality network connectivity and service. To fulfill this practical requirement, this paper extends the original WMN-RNP problem to a more realistic one that incorporates the service priority constraint, in which each mesh client is also associated with a service priority; the mesh clients with higher priorities than a threshold must be served as well.

Assume that the location and service priority of each mesh client are predefined. As for the problem of the WMN-RNP with service priority constraint (WMN-RNPSP for short), of

Manuscript received March 8, 2014; revised June 8, 2014; accepted July 13, 2014. This work was supported in part by the National Science Council of Taiwan under Grant NSC 101-2628-E-009-025-MY3 and Grant NSC 102-2221-E018-012-MY3, by the Guangdong University of Petrochemical Technology Internal Project under Grant 2012RC0106, and by the Educational Commission of Guangdong Province, China under Project 2013KJCX0131. (Corresponding author: Der-Jiunn Deng.)

C.-C. Lin is with the Department of Industrial Engineering and Management, National Chiao Tung University, Hsinchu 300, Taiwan (e-mail: cclin321@nctu.edu.tw).

L. Shu is with the Guangdong Provincial Key Laboratory of Petrochemical Equipment Fault Diagnosis, Guangdong University of Petrochemical Technology, Maoming 525000, China (e-mail: lei.shu@lab.gdupt.edu.cn).

D.-J. Deng is with the Department of Computer Science and Information Engineering, National Changhua University of Education, Changhua 500, Taiwan (e-mail: djdeng@cc.ncue.edu.tw).

Color versions of one or more of the figures in this paper are available online at <http://ieeexplore.ieee.org>.

Digital Object Identifier 10.1109/JSYST.2014.2341033

priority concern is how to find a placement of mesh routers in a rectangular deployment area in order to maximize two network performance measures: network connectivity (i.e., the size of the greatest component of the topology graph underlying the WMN) and client coverage (i.e., the number of clients within the radio coverage of mesh routers). Although this problem is a combinatorial optimization problem related to facility and location problems [6], the WMN-RNPSP problem is challenging owing to its following three features: the locations of mesh routers are not predetermined; each mesh router has a different-size radio coverage; and each mesh client with a different service priority is of priority concern. Inherited from the original WMN-RNP problems [17]–[19], the WMN-RNPSP problem is computationally intractable in general. Therefore, this paper presents a novel SA approach with momentum terms based on [20] to provide a highly promising solution to the above problem. The proposed SA approach increases the efficiency of the SA algorithm by additionally considering momentum terms, capable of improving the speed and accuracy of the original annealing schedules and preventing extreme changes in values of the acceptance probability function. In addition to the original neighbor selection scheme, three neighbor selection schemes are compared with the proposed SA approach. Analysis results demonstrates the outperformance of our proposed SA approach not only by discussing in detail how different parameters affect the performance but also by comparing our proposed SA approach with the original SA algorithm.

This paper contributes to optimizing the RNP in WMNs in the following ways.

- 1) The service priority constraint in the WMN-RNP problem is considered here, which is more realistic than that in previous works [12], [13], [15], [16];
- 2) A novel SA approach with momentum terms for the WMN-RNPSP problem is developed, capable of achieving convergence of the algorithm more efficiently and finding better solutions.
- 3) Time complexity of the proposed SA approach is analyzed theoretically.
- 4) Three neighbor selection schemes are considered in the proposed SA approach for comparison. Analysis results indicate that the proposed approach is highly effective in finding the optimal solutions.

II. PRELIMINARIES

Here, the basic settings of the original WMN-RNP problem are first introduced, and the WMN-RNPSP problem of concern is then mathematically formulated. The SA algorithm with momentum terms proposed in [20] is also reviewed.

A. WMN-RNP Problem

The WMN consists of mesh routers and mesh clients, in which each mesh client can only communicate with the node within the same radio coverage or any node that can be accessed via multihop router communications. Restated, a mesh client cannot communicate with other nodes in the network if it is not located within the radio coverage of a mesh router. For

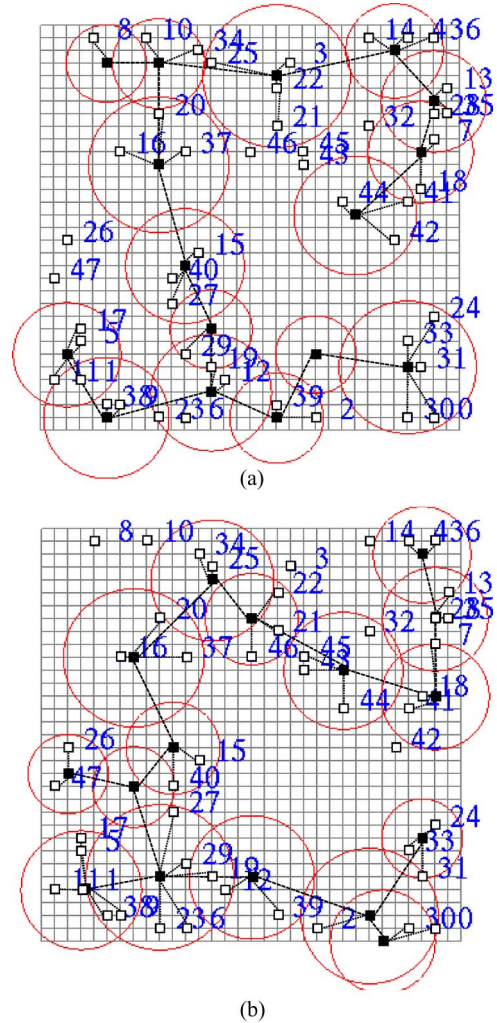


Fig. 1. Comparison of the experimental results between (a) our concerned WMN-RNPSP problem and (b) the previous WMN-RNP problem.

instance, Fig. 1(a) displays a WMN deployed in a grid area in which each mesh client (white node) is located at some grid point; in addition, each mesh router (black node) has different-size radio coverage (represented by a circle centered at the mesh router). Notably, all nodes must be placed only at grid points of the deployment area. The WMN-RNP problem [13], [15] focuses on how to find a placement of mesh routers in the grid deployment area in order to ensure that both *network connectivity* and *client coverage* are as large as possible.

To evaluate the above network performance measures, this paper establishes a **network topology graph $G = (V, E)$** based on the deployed locations of mesh routers [see Fig. 1(a)], in which **V denotes the set of all mesh routers and mesh clients**, and **E represents the set of edges**, which include the following two connections. First, for overlapped radio coverage of two mesh routers, there is an edge between the two mesh routers. Second, for a mesh client located within the radio coverage of a mesh router, there is an edge between the mesh client and the mesh router. **Network connectivity refers to the size of the greatest graph component of graph G** , whereas **client coverage refers to the number of covered mesh clients**. With these definitions, *network connectivity* and *client coverage* for the instance in Fig. 1(a) are 16 and 43, respectively.

B. WMN-RNP Problem With Service Priority Constraint

To satisfy the practical requirement of mesh clients in terms of nonuniformity, assume that each mesh client is associated with a service priority. Additionally, consider the service priority constraint in which the mesh client with a higher priority than a threshold must be served. A mathematical model for WMN-RNPSP is established as follows.

Consider a WMN with n mesh routers and m mesh clients deployed in a 2-D grid deployment area, in which the location of each mesh client is predefined. Meanwhile, the location of each mesh router must be determined. **The ability to determine a placement X of mesh routers of a WMN allows us to establish a graph $G_X = (V, E_X)$ where:**

- 1) $V = \{r_1, r_2, \dots, r_n, c_1, c_2, \dots, c_m\}$, where each r_i denotes a mesh router for $i \in \{1, 2, \dots, n\}$, and each c_j denotes a mesh client for $j \in \{1, 2, \dots, m\}$; let $R = \{r_1, r_2, \dots, r_n\}$ and $C = \{c_1, c_2, \dots, c_m\}$;
- 2) each mesh router $r_i \in R$ has radio coverage Υ_i , which can be viewed as a circle centered at node r_i with a different radius γ_i ;
- 3) each mesh client $c_j \in C$ has a service priority ω_j ;
- 4) according to placement X , if $\Upsilon_i \cap \Upsilon_k \neq \emptyset$ for any two mesh routers $r_i, r_k \in R$, then edge $(r_i, r_k) \in E_X$; and
- 5) according to **placement X , if $c_j \in \Upsilon_i$ for any mesh client $c_j \in C$ and any mesh router $r_i \in R$, then edge $(c_j, r_i) \in E_X$.**

Notably, for similarity, assume that two mesh routers can communicate with each other only if their radio coverage is overlapped. This assumption is acceptable because two mesh routers with overlapped radio coverage imply that their close geographical proximity so that they can communicate with each other.

With respect to placement X , assume that there are h subgraph components $G_X^1, G_X^2, \dots, G_X^h$ in G_X , i.e., $G_X = G_X^1 \cup G_X^2 \cup \dots \cup G_X^h$, and $G_X^a \cap G_X^b = \emptyset$ for $a, b \in \{1, \dots, h\}$. **The network connectivity is calculated based on the size of the greatest subgraph component,** which is expressed as follows:

$$\phi(G_X) = \max_{a \in \{1, \dots, h\}} \{|G_X^a|\}.$$

The client coverage can be expressed as follows:

$$\psi(G_X) = |\{j; d_X(c_j) > 0 \text{ for } j \in \{1, \dots, m\}\}|$$

where $d_X(c_j)$ denotes the degree of node c_j in graph G_X . **This paper attempts to maximize the two network performance measures simultaneously as follows:**

$$f(G_X) = \lambda \cdot \phi(G_X)/(n + m) + (1 - \lambda) \cdot \psi(G_X)/m \quad (1)$$

where λ represents the weighting scale in the range $[0, 1]$, and it controls the balance between the two terms of the objectives. Notably, the denominator of each term of the equation is used for normalization.

With these notations, the WMN-RNPSP problem can be stated as follows:

WMN-RNPSP

INSTANCE: A number κ and a WMN deployed in a 2-D $W \times H$ grid area where each mesh client is located at a particular grid point.

QUESTION: Find a placement X of mesh routers of the WMN problem such that $f(G_X)$ for the underlying graph G_X is maximized. Meanwhile, the mesh clients with the top κ service priorities must be served, and each mesh router must be placed at a grid point.

Fig. 1 compares the experimental results of the WMN-RNPSP problems of concern in this paper with the previous WMN-RNP for a WMN with 16 mesh routers (black nodes) and 48 mesh clients (white nodes) labeled by their service priority ordering, in which a smaller label number represents a higher priority. Let $\kappa = m/3$, i.e., the mesh clients with the top $48/3 = 16$ service priorities (labeled by 0 to 15) must be served. Note that κ can be any number, and we set it to be $(m/3)$ in this example. Analysis results for the previous WMN-RNP problem in Fig. 1(b) indicate that the mesh clients labeled by 3, 8, 10, and 14 are not serviced even if they have higher priorities. As for the experimental results for the WMN-RNPSP problem of concern in this paper [see Fig. 1(a)], all the mesh clients labeled by 0 to 15 are serviced, although some mesh clients with lower priorities are still not served.

C. SA With Momentum Terms

SA is a metaheuristic algorithm like the genetic algorithm (GA), which can solve various combinatorial optimization problems. As the GA has been applied to various applications (e.g., [21]–[23]), some recent applications of SA in a variety of fields include those in [24]–[26]. SA simulates the cooling process of metals by heating and cooling the metals to increase the size of crystals and reduce defects. Initially, an encoding method must be designed to represent the solution of the concerned problem as a *state* of the metals in SA and to establish the relationship between the objective function of the concerned problem and the *energy* model of the metals. Consequently, the optimal solution corresponds to a state with the lowest energy. In SA, the *annealing schedule* and the *Metropolis rule* significantly influence the performance of SA. Let T_k denote the temperature of the k th iteration. Three conventionally adopted annealing schedules [20] that update the temperature per iteration are stated as follows.

- 1) *Geometric*: $T_{k+1} = \alpha \cdot T_k$, where α denotes a cooling parameter ranging from 0.9 to 0.999.
- 2) *Logarithmic*: $T_{k+1} = c / \log(b_0 + k)$, where c represents a value determined by many experimental trials and depends on the concerned problem, and b_0 is a base;
- 3) *Boltzmann*: $T_{k+1} = T_0 / \log(1 + k)$, where T_0 denotes the initial temperature, i.e., $T_0 = T_h$.

The SA algorithm is also characterized by the *Metropolis rule*, which considers an acceptance probability function that overcomes the local optimal problem and leads the system toward the global optimal solution. To allow escaping from the local optimal solution, the rule allows for acceptance of an undesired state with the Boltzmann acceptance probability $P(\Delta\mathcal{E}) = e^{-\Delta\mathcal{E}/(B \cdot T_k)}$, where B denotes the Boltzmann constant and is generally set to one, $\Delta\mathcal{E} = \mathcal{E}'_k - \mathcal{E}_k$ for the minimization problem (in which \mathcal{E}_k and \mathcal{E}'_k represent the energy values of the current state and neighboring state, respectively), and $\Delta\mathcal{E} = \mathcal{E}_k - \mathcal{E}'_k$ for the maximization problem.

A previous work [20] suggested adding momentum terms to SA to improve cooling rate and to prevent extreme changes in values on the acceptance probability function, allowing for a more efficient solution of the problem and higher accuracy of the solution. For an annealing schedule, to avoid extreme cooling and increase the efficiency of deriving better solutions, three annealing schedules were proposed by adding momentum terms to the above three annealing schedules, respectively, as follows.

- 1) *Hybrid*: $T_{k+1} = T_k - \alpha \cdot T_k - k \cdot (T_k - T_{k-1})/e^k$.
- 2) *Extended Logarithmic*: $T_{k+1} = c/\log(T_0 + k) - k/e^k - \sqrt{\log(k)}$.
- 3) *Extended Boltzmann*: $T_{k+1} = T_0/\log(1+k) - \log(1+k)$.

Further details of those designs can be found in [20].

As for the Metropolis rule, the extended Boltzmann acceptance probability was proposed based on the notion of adding momentum terms to the Boltzmann acceptance probability as follows:

$$P(\Delta\mathcal{E}) = e^{-\Delta\mathcal{E}/(B \cdot T_k)} \quad (2)$$

where $\Delta\mathcal{E} = (\mathcal{E}'_k - \mathcal{E}_k) - \beta \cdot B \cdot T_k \sqrt{\mathcal{E}'_k - \mathcal{E}_k}$ for minimization problem, or $\Delta\mathcal{E} = (\mathcal{E}_k - \mathcal{E}'_k) - \beta \cdot B \cdot T_k \sqrt{\mathcal{E}_k - \mathcal{E}'_k}$ for maximization problem, where we recall that \mathcal{E}_k and \mathcal{E}'_k are the energy values of current state and neighboring state, respectively, and β is a running time parameter that depends on the annealing schedule and initial temperature. Notably, $\Delta\mathcal{E}$ is always no less than zero because the neighboring state is accepted if $\Delta\mathcal{E} < 0$.

III. OUR SA APPROACH WITH MOMENTUM TERMS FOR THE WMN-RNPSP PROBLEM

Here, the proposed SA approach is described in detail with momentum terms for the WMN-RNPSP problem. Basic components of the SA approach (i.e., solution representation, fitness function, neighbor selection scheme, repairing function, and acceptance criterion) are introduced. Details of the SA algorithm are provided as well.

A. Solution Representation

The solution to the WMN-RNPSP problem of concern in this paper is a placement of m mesh routers in a 2-D $W \times H$ grid deployment area, whose lower left corner is place at the origin of an $x \times y$ plane. Restated, the (x, y) coordinates of the m mesh routers should be determined for each candidate solution. Therefore, a state (solution) of SA for the WMN-RNPSP problem can be expressed by $X = (x_1, x_2, \dots, x_{2n})$ where (x_{2i-1}, x_{2i}) denotes the (x, y) -coordinate of mesh router r_i for $i = 1, 2, \dots, n$.

Additionally, each iteration of SA maintains the optimum state found so far and, hence, records it in the vector $P = (p_1, p_2, \dots, p_{2n})$, along with its energy (objective) value $f(P)$. Notably, each node is restricted to be placed at a grid point; hence, x_i and p_i are integers for any $i \in \{1, \dots, n\}$.

Since all of the mesh routers are placed within a $W \times H$ area, the following constraint is obtained: $\forall i \in \{1, 2, \dots, n\}$,

$$0 \leq x_{2i-1} \leq W \quad 0 \leq x_{2i} \leq H. \quad (3)$$

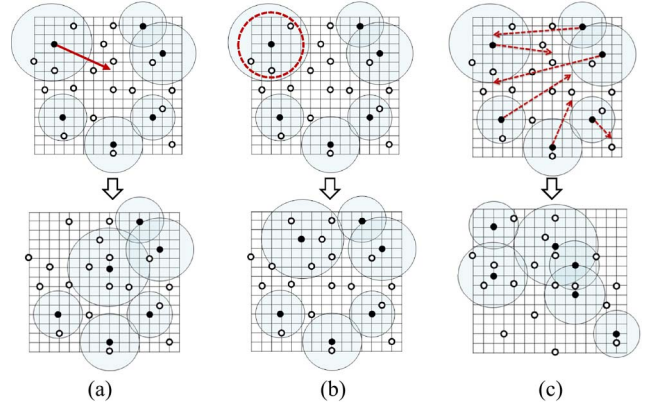


Fig. 2. Proposed three neighbor selection schemes: (a) standard, (b) local, and (c) random.

B. Fitness Function

In the setting of the original SA, a state of metals has an energy value corresponding to the objective value of the solution that the state represents. Although the original SA attempts to find the state with the minimal energy value, the WMN-RNPSP problem of concern in this paper focuses on obtaining a solution with the maximal objective value. For clarity, by use of the terminology of evolutionary computation, the proposed SA approach assumes that each state has a *fitness* value rather than an energy value. Therefore, this paper attempts to find a state with the fittest value, i.e., the maximal fitness value. Doing so makes us to simply allow the fitness function to be the objective function as follows. Consider a state that represents a candidate placement X of mesh routers. A topology graph G_X underlying the WMN deployment can be established, as described in Section II-B. As aforementioned, the problem of concern in this paper attempts to maximize the size of the greatest subgraph component $\phi(G_X)$ and the client coverage $\psi(G_X)$ simultaneously. Hence, SA searches for a state that maximizes the fitness function $f(G_X)$ for G_X in (1).

C. Neighbor Selection

Neighbor selection plays an important role in finding the optimal state of the metals. The neighboring state is generally transformed from the current state and differs only slightly from the current state. For experimental diversity, consider the following three neighbor selection schemes.

- 1) *Standard*: Randomly select a mesh router in the current state and then place it at an arbitrary grid point [e.g., see Fig. 2(a)].
- 2) *Local*: Select a mesh router randomly, and then place it at an arbitrary grid point within its local area [e.g., see Fig. 2(b)].
- 3) *Random*: All of the mesh routers are relocated randomly [e.g., see Fig. 2(c)].

Notably, more than just a slight modification, the random neighbor selection scheme changes the locations of all of the mesh routers. Hence, comparing this scheme with the other two schemes with small-scale modification is of relevant interest.

D. Repairing Function

Any of the three neighbor selection schemes described earlier may destroy the solution feasibility. Restated, the service priority constraint is violated as some of the mesh clients with the top κ service priorities are not served. Maintaining the solution feasibility in each iteration of the SA algorithm depends on our ability to design how to rectify this infeasibility. As aforementioned, each mesh client c_j is associated with a service priority ω_j , and a smaller ω_j value implies a higher priority. This paper attempts to repair the operator by moving the mesh routers that cover low-priority mesh clients to serve those that must be served but are not served yet.

Our algorithm for the repairing operator is stated in detail in Algorithm 1, which is explained in the following. Line 1 considers each mesh client c_j that must be served but is not yet served. Line 2 then allows S to be the set of mesh clients that are covered but do not belong to those with the top κ service priorities and are sorted in a decreasing order of service priorities (i.e., lowest priority to highest priority). To determine whether the job of covering the concerned mesh client c_j is complete, line 3 uses a flag variable called `isDone`, which is set to false initially.

Algorithm 1 REPAIRING

```

1: for each mesh client  $c_j$  that must be served but is not yet
   do
2:   let  $S$  denote a list of mesh clients in which they are
     covered but do not belong to those with the top  $\kappa$  service
     priorities; they are sorted in a decreasing order of
     service priorities (i.e., lowest priority to highest priority)
3:    $isDone \leftarrow false$ 
4:   for each mesh client  $c_t$  in list  $S$  do
5:     let  $R_\ell$  denote the set of the mesh routers that cover
       mesh client  $c_t$ 
6:     for each mesh router  $r_i$  in  $R_\ell$  do
7:       find an available grid point  $g_j$  that is the closest to  $c_j$ 
8:       if the placement of  $r_i$  at grid point  $g_j$  does not violate
         the service priority constraint then
9:         place mesh router  $r_i$  at grid point  $g_j$  to serve mesh
           client  $c_j$ 
10:       $isDone \leftarrow true$ 
11:      break the for loop
12:     end if
13:   end for
14:   if  $isDone = true$  then break the for loop
15: end for
16: if  $isDone = false$  then discard the solution
17: update the mesh clients that must be served but is not yet
18: if all the mesh clients are served then return the solution
19: end for

```

We repeat the FOR loop of lines 4–15 until each mesh client c_t in S is considered. Notably, since S is a list of mesh clients from the lowest priority to the highest priority, c_t is a mesh client in S with the lowest priority that is not yet considered. Line 6 finds the mesh routers R_ℓ that cover mesh client c_t . Then,

the FOR loop of lines 6–13 is repeated until each mesh router in R_ℓ is considered. In each iteration of the loop, lines 7 and 8 consider whether to move mesh router r_i to serve mesh client c_j (by placing r_i at an available grid point that is the closest to c_j). The move is accomplished if it does not lead to any new violation of the service priority constraint (i.e., the mesh clients that were served by mesh router r_i originally are still served after the move). Since the move is executed in the most inner loop, the flag variable `isDone` is allowed to be true in line 11.

In line 14, if `isDone` = *true* (i.e., the job of serving mesh client c_j is done), break up the FOR loop of lines 4–15 until R_ℓ is empty. In line 16, if `isDone` = *false* (i.e., mesh client c_j is still not served), meaning that the feasibility of the solution cannot be solved, then the solution is discarded. Lines 17 and 18 update the solution and return it as the final solution if there is no constraint violation.

Notably, Algorithm 1 may lead to a situation in which, although some low-priority mesh clients are not covered, it can still guarantee the solution feasibility.

Consider Fig. 1(a) as an example, in which mesh clients are labeled by 0–47; in addition, the mesh clients labeled by 26, 43, 45, 46, and 47 are not served. By assuming that the mesh clients with the top 26 service priorities must be served, mesh client #26 (i.e., c_j in line 1 of Algorithm 1) must be served. Line 2 creates a list S that includes mesh clients #44, #42, #41, ..., #27, #28, i.e., all of the mesh clients exclusive of #26, #43, #45, #46, and #47. Line 4 finds mesh #44 with the lowest priority. Line 5 indicates that R_ℓ includes the mesh router between mesh clients #44 and #42 in Fig. 1(a). Lines 7–12 move the mesh router to serve mesh client #26 by placing it at one of the four grid points near mesh client #26. The algorithm is completed since it serves mesh client #26 successfully and does not induce any new violation.

The time complexity of Algorithm 1 is analyzed as follows.

Lemma 1: The worst-case upper bound of the time complexity of Algorithm 1 is $O(\kappa \cdot (m - \kappa) \cdot (m + n) \cdot n)$.

Proof: Line 1 in Algorithm 1 considers at most κ mesh clients because an attempt is made to serve at most κ mesh clients. Hence, the main loop has at most κ iterations. Relatively, in line 2, S may include the remaining $m - \kappa$ mesh clients at most, and hence, $|S| \leq m - \kappa$. Notably, despite an attempt to sort S in line 2, it does not need to be sorted because the data structure containing all mesh clients in a decreasing order of service priorities was known originally. Restated, line 2 can be completed in $O(m - \kappa)$ time. Next, line 3 is completed in $O(1)$ time.

Line 4 considers each mesh client in S , i.e., there are $O(m - \kappa)$ iterations. Next, in lines 5 and 6, R_ℓ contains n mesh routers in the worst case, although the worst case does not occur often in practice. Line 7 computes the available closest grid point to c_j in $O(m + n)$ time because the maximum number of the neighboring grid points of c_j that are occupied by other mesh routers and clients is bounded by $O(m + n)$.

Lines 8–12 and Line 14 are completed in $O(1)$ time. Lines 16–18 can be completed in $O(m)$ time.

In light of the above discussion, the time complexity of Algorithm 1 can be calculated as $O(\kappa \cdot ((m - \kappa) + (m - \kappa) \cdot n \cdot (m + n) + m)) = O(\kappa \cdot (m - \kappa) \cdot (m + n) \cdot n)$. ■

E. Acceptance Criterion

After neighbor selection and repairing, the acceptance criterion for the neighboring state is based on the difference of the fitness values between the current state X and the neighboring state X' as follows.

- 1) If $f(X') - f(X) \geq 0$, then X' is accepted.
- 2) If $f(X') - f(X) < 0$, then X' is accepted based on the extended Boltzmann acceptance probability function in (2), where $\Delta\mathcal{E}$ can be rewritten as $(f(X) - f(X')) - \beta \cdot B \cdot T_k \sqrt{f(X) - f(X')}$.

F. Proposed SA Algorithm

The proposed SA algorithm works with the current state X , which is a $2n$ -length vector that represents a candidate solution of the WMN-RNPSP problem. First, each pair (x_{2i}, x_{2i+1}) in X is initialized to be a random position in the grid deployment area. The proposed SA algorithm then finds a neighboring state X' of the current state X and probabilistically determines whether the system moves to the neighboring state X' or remains in the current state X . In doing so, the system can move to a state of lower energy. This step is repeated until the system reaches a state that is acceptable for the problem of concern in this paper or until the maximum number of iterations is achieved.

Algorithm 2 OUR SA WITH MOMENTUM TERMS

- 1: initialize the current state $X = (x_1, x_2, \dots, x_n)$ randomly where x_{2i-1} is an integer in the range $[0, W]$ and x_{2i} is an integer in the range $[0, H]$ for each $i \in \{1, 2, \dots, n\}$, and calculate its fitness value $f(X)$
- 2: $P \leftarrow X$ and $f(P) \leftarrow f(X)$
- 3: initialize temperatures T_h and T_ℓ , and let temperature $T_0 \leftarrow T_h$
- 4: $k \leftarrow 0$
- 5: **while** $T_k > T_\ell$ and $k < \eta$ where η is the maximal iteration number **do**
- 6: **repeat**
- 7: generate the neighboring state X' by a neighbor selection scheme (which may be one of the standard, local, and random neighbor selection schemes described in Section III-C)
- 8: if X' violates the service priority constraint, then repair its infeasibility as described in Section III-D
- 9: calculate the fitness value $f(X')$ of neighboring state X'
- 10: **if** $f(X') \geq f(X)$ **then**
- 11: $X \leftarrow X'$ and $f(X) \leftarrow f(X')$
- 12: **if** $f(X) > f(P)$ **then**
- 13: $P \leftarrow X$ and $f(P) \leftarrow f(X)$
- 14: **end if**
- 15: **else**
- 16: **if** $\text{rand}() < \exp(-\Delta\mathcal{E}/(B \cdot T_k))$ **then**
- 17: $X \leftarrow X'$ and $f(X) \leftarrow f(X')$
- 18: **end if**
- 19: **end if**

- 20: **until** there have been consecutive τ times of rejecting the neighboring state or the maximal iteration of the inner loop is achieved
 - 21: update temperature according a annealing schedule (which may be one of the hybrid, extended logarithmic, and extended Boltzmann annealing schedules described in Section II-C)
 - 22: $k \leftarrow k + 1$
 - 23: **end while**
 - 24: output P as the solution
-

Algorithm 2 states the proposed SA algorithm. The key steps of Algorithm 2 are explained as follows. Lines 1–4 are the initialization of current state X , best state P obtained so far, their fitness values, highest temperatures T_h , lowest temperature T_ℓ , initial temperature T_0 , and initial iteration number k . Line 1 initializes the current state X randomly under constraint (3), and calculates its fitness value by (1). Line 2 assigns the current state X and its fitness value $f(X)$ to the best state P found so far and its corresponding fitness value $f(P)$, respectively. Lines 3 initializes temperatures T_h and T_ℓ and assigns T_h to the initial temperature T_0 .

Lines 5–23 are the main loop (outer loop) of the SA algorithm, which is repeated until the number of iterations k is greater than the maximum iteration number η or the current temperature T_k drops to the lowest temperature T_ℓ . At a fixed temperature T_k , the inner loop in lines 6–20 determines whether to accept the neighboring state until the *equilibrium detection condition* is achieved, i.e., there have been consecutive τ times of rejecting the neighboring state (i.e., the solution has not been modified for a number of τ times) or the maximum number of the inner loops (Line 20) has been achieved. Line 7 generates the neighboring state X' by a neighbor selection scheme described in Section III-C. Line 8 checks whether the neighboring state violates the service priority constraint. If true, the repairing operation described in Section III-D is applied. Next, line 9 calculates the fitness value $f(X')$ of X' . Once a better state is found, the current state is replaced by the neighboring state X' ; in addition, the best state P found so far and its fitness value $f(P)$ are updated in lines 10–14. Otherwise (i.e., the neighboring state X' is worse), a nonzero extended Boltzmann acceptance probability is considered to accept the worse neighboring state in lines 15–19. Line 21 updates the temperature according to an annealing schedule described in Section II-C. Finally, line 24 outputs the final solution represented by P upon completion of the SA algorithm.

Before the time complexity of Algorithm 2 is analyzed, the following lemma is obtained.

Lemma 2: Given a placement X of mesh routers, the fitness value $f(G_X)$ with respect to X can be computed in $O(m \cdot n)$ time.

Proof: The fitness value is calculated by first establishing the topology graph G_X underlying the concerned WMN instance in $O(m \cdot n)$ time. To do so, whether each of the m mesh clients is located within the radio coverage of each of the n mesh routers is verified. Once graph G_X is established, the size of the greatest component $\phi(G_X)$ is obtained in $O(1)$

time. Next, $O(m)$ time is taken to verify whether each of the m mesh clients is covered; hence, the client coverage $\psi(G_X)$ is obtained in $O(m)$ time. Therefore, $f(G_X)$ can be computed in $O(m \cdot n + m) = O(m \cdot n)$ time. ■

The time complexity of the main loop (i.e., lines 6–20) in Algorithm 2 is analyzed as follows.

Theorem 1: Each iteration of the loop of lines 6–20 in Algorithm 2 can be computed in $O(\kappa \cdot (m - \kappa) \cdot (m + n) \cdot n)$ time.

Proof: First, the standard, local, and random neighbor selection schemes in line 7 can obviously be computed in $O(1)$, $O(1)$, and $O(n)$ times, respectively. By Lemma 1, Line 8 is completed in $O(\kappa \cdot (m - \kappa) \cdot (m + n) \cdot n)$ time. By lemma 2, Line 9 is completed in $O(m \cdot n)$ time. Each of the other lines in the concerned loop is an assignment or comparative instruction and hence can be done in $O(1)$ time. ■

IV. IMPLEMENTATION AND ANALYSIS RESULTS

Here, the proposed SA approach to the WMN-RNPSP problem is implemented. The experimental data and environment are described first, and then, a comprehensive experimental analysis is conducted under different neighbor selection schemes, annealing schedules, acceptance probability functions, and distributions of mesh clients.

A. Data and Environment

Let $U(a, b)$ denote the uniform distribution over $[a, b]$. By analogy with [13], the following three cases are considered (as also used in our previous work in [16]).

Case 1: There are 16 mesh routers ($m = 16$) and 48 mesh clients ($n = 48$) on a 32×32 grid area ($W = H = 32$). Each mesh router is associated with a circular radio coverage with radius following a uniform distribution $U(3, 6)$. Meanwhile, the position of each mesh client is generated following a uniform distribution $U(0, 32)$ or a normal distribution $N(16, 16/3)$. Temperatures $T_h = 100$ and $T_\ell = 1$.

Case 2: There are 32 mesh routers ($m = 32$) and 96 mesh clients ($n = 96$) on a 64×64 grid area ($W = H = 64$). Each mesh router is associated with a circular radio coverage with radius following a uniform distribution $U(4\sqrt{2} - 2, 8\sqrt{2} - 2)$. Meanwhile, the position of each mesh client is generated following a uniform distribution $U(0, 64)$ or a normal distribution $N(32, 32/3)$. Temperatures $T_h = 50$ and $T_\ell = 1$.

Case 3: There are 64 mesh routers ($m = 64$) and 192 mesh clients ($n = 192$) on a 128×128 grid area ($W = H = 128$). Each mesh router is associated with circular radio coverage with radius following a uniform distribution $U(7, 14)$. Meanwhile, the position if each mesh client is generated following a uniform distribution $U(0, 128)$ or a normal distribution $N(64, 64/3)$. Temperatures $T_h = 50$ and $T_\ell = 1$.

Notably, the deployment area is a grid, implying that each coordinate is an integer. For each case, five instances are generated, in which mesh clients are deployed in the area according to a uniform or normal distribution. Our experiments

TABLE I
PERFORMANCE OF USING DIFFERENT NEIGHBOR SELECTION SCHEMES ON THE ORIGINAL SA AND OUR PROPOSED SA WITH MOMENTUM TERMS FOR 32×32 , 64×64 , AND 128×128 GRID CASES

| Case | Momentum terms | Standard | Local | Random |
|-----------------------|----------------|----------|----------|----------|
| 32×32 grid | without | 0.955385 | 0.743010 | 0.744469 |
| | with | 0.982656 | 0.788635 | 0.783781 |
| 64×64 grid | without | 0.923776 | 0.873375 | 0.876479 |
| | with | 0.999229 | 0.879516 | 0.871833 |
| 128×128 grid | without | 0.884500 | 0.859797 | 0.860487 |
| | with | 0.981529 | 0.866550 | 0.868177 |

apply the following parameter settings for the SA: $\lambda = 0.3$ (i.e., weighting parameter of objective function), $\eta = 200$ (number of iterations), and $\tau = 20$ (i.e., allowed number of consecutive times of rejecting the neighboring state). Additionally, $\rho = 50$ independent runs are performed to avoid fortuitous results, explaining why averaged results are used. The proposed SA algorithm is tested on a PC with an Intel Core i7-3770 CPU and 16-GB memory. Under such a setting, the average running times for executing an instance of 32×32 , 64×64 , and 128×128 grid cases are 0.646, 12.864, and 56.003 s, respectively, implying that the proposed SA approach can cope with the concerned problem efficiently.

B. Experimental Results Under Different Neighbor Selection Schemes

Performance of the proposed algorithm under different neighbor selection schemes (see Section III-C) is evaluated by running 50 times of SA with or without momentum terms for each problem case under different neighbor selection schemes. The average of all the outputted fitness values in Table I is recorded as well. Notably, unless stated otherwise, the following basic settings of the SA components are as follows: the SA algorithm without momentum terms uses the geometric annealing schedule and the Boltzmann acceptance probability. Meanwhile, the SA algorithm with momentum terms uses the hybrid annealing schedule and the extended Boltzmann acceptance probability. Table I reveals that the cases using the standard neighbor selection scheme always generate better solutions than those in the other cases.

Next, solution convergence of the proposed SA algorithm is observed by plotting the outputted fitness values versus the number of iterations of the main loop of our proposed SA algorithm for an instance of each grid case in Fig. 3. Fig. 3(a) shows the convergence trend for the 32×32 grid case indicating that the standard neighbor selection scheme converges very close to one (i.e., the best fitness value) at the 40th iteration and demonstrates a very good convergence performance. Meanwhile, the local and random neighbor selection schemes improve the solutions gradually after the first iteration, finally obtaining relatively worse solutions.

Fig. 3(b) shows the convergence trend for the 64×64 grid case. From this, we infer that the standard neighbor selection scheme performs better than the other two schemes. A similar inference can also be made for the case for the 128×128 grid case in Fig. 3(c). However, the gap between the Standard and the other two neighbor selection schemes in Fig. 3(b)

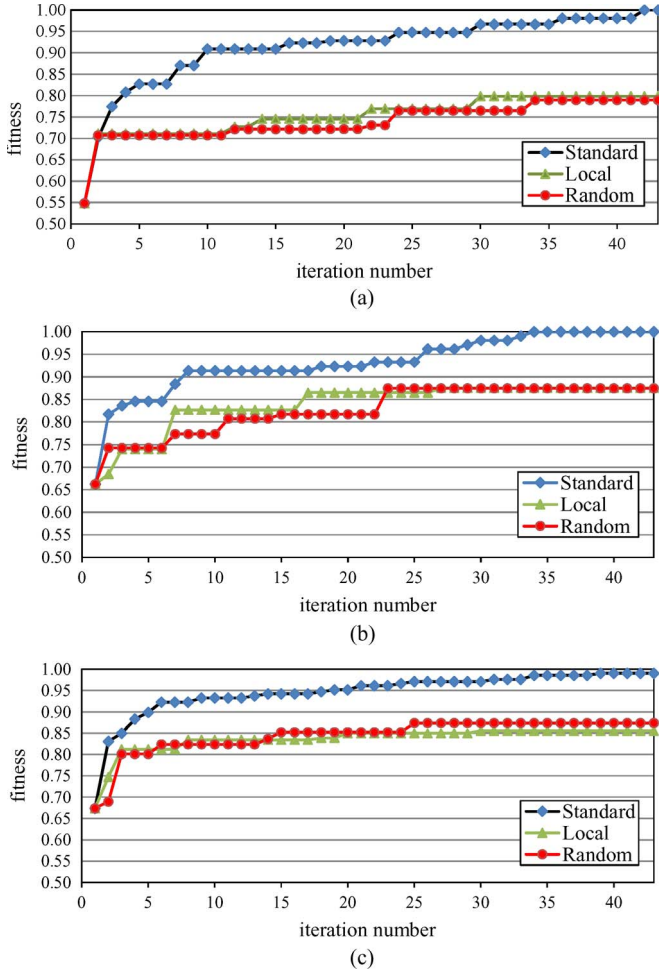


Fig. 3. Convergence trend of our proposed SA under different neighbor selection schemes for (a) 32×32 , (b) 64×64 , and (c) 128×128 grid cases.

[respectively, Fig. 3(c)] becomes narrower than that in Fig. 3(a). This finding suggests that different neighbor selection schemes do not significantly influence larger grid cases.

C. Experimental Results With Different Annealing Schedules and Acceptance Probability Functions

This paper also attempts to understand how using different annealing schedules and acceptance probability functions influences the resulting fitness values. A thorough analysis is performed for all possible combinations of annealing schedules and acceptance probability functions in Table II. This table summarizes the experimental results of the proposed SA algorithm using Boltzmann and extended Boltzmann acceptance probability functions, respectively, under six annealing schedules (mentioned in Section II) for each grid case. Notably, each entry in Table II is computed by the average of running five instances with uniformly distributed mesh clients for the proposed SA approach.

The experimental results of the Boltzmann probability acceptance function in Table II indicate that the geometric annealing schedule performs better than the others for 32×32 and 64×64 grid cases, particularly for the 32×32 grid case. Meanwhile, the extended logarithmic annealing schedule performs better for

TABLE II
RESULTANT FITNESS VALUES OF OUR PROPOSED SA USING BOLTZMANN AND EXTENDED BOLTZMANN ACCEPTANCE PROBABILITY FUNCTIONS, RESPECTIVELY, UNDER DIFFERENT ANNEALING SCHEDULES FOR THREE GRID CASES

| Acceptance probability | Annealing schedule | 32×32 | 64×64 | 128×128 |
|------------------------|----------------------|----------------|----------------|------------------|
| Boltzmann | Geometric | 0.949562 | 0.928870 | 0.882378 |
| | Logarithmic | 0.769073 | 0.892849 | 0.870396 |
| | Boltzmann | 0.766104 | 0.895083 | 0.866521 |
| | Hybrid | 0.870500 | 0.852052 | 0.831609 |
| | Extended Logarithmic | 0.765312 | 0.896604 | 0.866997 |
| Expanded Boltzmann | Extended Boltzmann | 0.763875 | 0.895531 | 0.867477 |
| | Geometric | 0.982292 | 0.962144 | 0.986125 |
| | Logarithmic | 0.981375 | 0.967908 | 0.985766 |
| | Boltzmann | 0.985792 | 0.977908 | 0.962916 |
| | Hybrid | 0.978687 | 0.945529 | 0.958355 |
| | Extended Logarithmic | 0.983083 | 0.953463 | 0.986221 |
| | Extended Boltzmann | 0.982406 | 0.964149 | 0.962278 |

the 128×128 grid case. Experimental results under extended Boltzmann probability acceptance function in Table II indicate that almost all annealing schedules can perform better than those under the Boltzmann probability acceptance function. We thus conclude that the extended Boltzmann acceptance probability function of the novel SA performs better.

D. Experimental Results of Different Distributions of Mesh Clients

This paper also evaluates the performance of the proposed SA algorithm for different problem instances. As aforementioned, mesh clients are distributed in the deployment area based on a uniform or normal distribution function. Tables III summarizes all of the problem instances for all cases, with each one having four columns that store the best fitness value, an average fitness value, the worst fitness value, and the standard deviation of fitness values of each instance; ten rows contain five instances with uniform distribution and five instances with normal distribution. The average of each column is stored at the bottom row of Table III, indicating that the proposed SA approach performs excellently for various grid cases. Particularly for the 32×32 and 64×64 grid cases, the best fitness values for nearly all of the instances are optimal. Restated, the proposed SA approach for small-size and middle-size cases had a high probability of achieving the optimal solutions for both network connectivity and client coverage.

To visualize the placement results, this paper implements a visualization user interface to show the solution placement. For instance, if the effectiveness of the proposed SA algorithm in achieving the optimality for the 32×32 and 64×64 grid cases is of interest, the validity of the solutions can be verified by visualizing their solution placements in Fig. 4(a) and (b), respectively. In these figures, each white node is a mesh client and is labeled by its priority ordering; each black node is a mesh router, and the circle centered at each mesh router is its radio coverage. Fig. 4 reveals that each white mesh client is covered, and the underlying topology graph due to overlapped radio coverage is connected. Hence, the solution correctness is verified via visualization.

TABLE III
STATISTICS FOR THE THREE GRID CASES

| 32 × 32 grid case | | | | |
|---------------------|----------|----------|-----------|-----------|
| instance | Best | Mean | Worst | SD* |
| Uniform_inst 1 | 1.000000 | 0.970719 | 0.932812 | 0.017754 |
| Uniform_inst 2 | 1.000000 | 0.990750 | 0.961458 | 0.011835 |
| Uniform_inst 3 | 1.000000 | 0.978708 | 0.942188 | 0.017179 |
| Uniform_inst 4 | 1.000000 | 0.987958 | 0.942708 | 0.013422 |
| Uniform_inst 5 | 0.985937 | 0.958458 | 0.922917 | 0.014834 |
| Normal_inst 1 | 1.000000 | 0.996344 | 0.817188 | 0.025854 |
| Normal_inst 2 | 1.000000 | 0.995781 | 0.827083 | 0.024931 |
| Normal_inst 3 | 1.000000 | 0.978031 | 0.922917 | 0.020199 |
| Normal_inst 4 | 1.000000 | 0.975292 | 0.922917 | 0.023592 |
| Normal_inst 5 | 1.000000 | 0.972958 | 0.922917 | 0.025047 |
| average | 0.998594 | 0.9805 | 0.9115105 | 0.0194646 |
| 64 × 64 grid case | | | | |
| instance | Best | Mean | Worst | SD* |
| Uniform_inst 1 | 1.000000 | 0.962948 | 0.901562 | 0.030137 |
| Uniform_inst 2 | 1.000000 | 0.969005 | 0.874740 | 0.029385 |
| Uniform_inst 3 | 0.990365 | 0.951599 | 0.911719 | 0.022636 |
| Uniform_inst 4 | 0.983333 | 0.931099 | 0.865104 | 0.032537 |
| Uniform_inst 5 | 0.954427 | 0.876341 | 0.807552 | 0.033011 |
| Normal_inst 1 | 1.000000 | 0.998073 | 0.913281 | 0.012312 |
| Normal_inst 2 | 1.000000 | 0.998849 | 0.944792 | 0.007808 |
| Normal_inst 3 | 1.000000 | 0.989469 | 0.738542 | 0.041472 |
| Normal_inst 4 | 1.000000 | 0.989016 | 0.882552 | 0.026658 |
| Normal_inst 5 | 1.000000 | 0.989802 | 0.877344 | 0.028532 |
| average | 0.991215 | 0.965541 | 0.868067 | 0.025713 |
| 128 × 128 grid case | | | | |
| instance | Best | Mean | Worst | SD* |
| Uniform_inst 1 | 0.990365 | 0.960885 | 0.879688 | 0.015012 |
| Uniform_inst 2 | 0.980729 | 0.960461 | 0.937370 | 0.010884 |
| Uniform_inst 3 | 0.985547 | 0.953370 | 0.908594 | 0.015991 |
| Uniform_inst 4 | 0.977214 | 0.932828 | 0.869922 | 0.020921 |
| Uniform_inst 5 | 0.995182 | 0.979461 | 0.959115 | 0.008762 |
| Normal_inst 1 | 1.000000 | 0.961464 | 0.879688 | 0.015941 |
| Normal_inst 2 | 0.985547 | 0.969656 | 0.942318 | 0.010350 |
| Normal_inst 3 | 0.980729 | 0.958208 | 0.892969 | 0.017861 |
| Normal_inst 4 | 1.000000 | 0.981003 | 0.900130 | 0.020739 |
| Normal_inst 5 | 0.969922 | 0.944716 | 0.791927 | 0.024531 |
| average | 0.986524 | 0.960205 | 0.896172 | 0.016099 |

* SD denotes standard deviation.

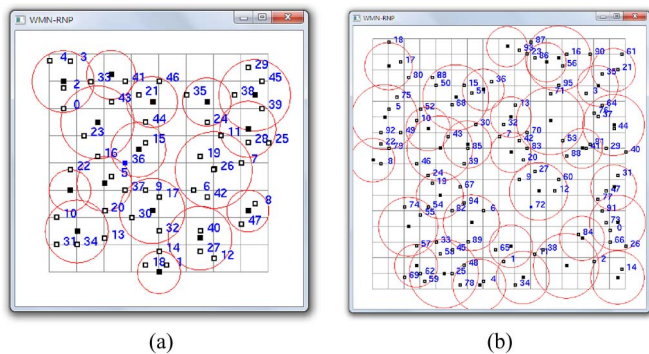


Fig. 4. Visualization of the WMNs for (a) 32 × 32 and (b) 64 × 64 grid cases, where it should be noticed that each gray grid represents a 4 × 4 grid.

V. CONCLUSION AND FUTURE WORK

This paper has presented an SA approach with momentum terms to optimize the placement of mesh routers with service priority constraint in WMNs. This paper has significantly

contributed to addressing a more realistic problem, in which the service priority constraint is added and an SA approach with momentum terms is provided to increase the speed and accuracy of the original SA. Additionally, the theoretical time complexity of the proposed SA approach is also provided. Analysis results demonstrate that the proposed SA approach performs well.

For different grid cases, the most effective strategies of the annealing schedule and acceptance probability function are identified. Analysis results further demonstrate that the Boltzmann schedule with extended Boltzmann probability function is the most effective strategy for 32 × 32 and 128 × 128 grid cases. Meanwhile, the geometric model with the extended Boltzmann probability function is the most effective strategy for 64 × 64 grid case. Moreover, the proposed SA algorithm is an effective method for the concerned problem, owing to its ability to achieve the connectivity of the entire network and cover nearly all mesh clients in various grid cases.

Efforts are underway in our laboratory to solve the dynamic version of the concerned problem and consider the optimization of other objectives simultaneously (e.g., minimum number of mesh routers and minimum traffic) in order that the problem is more realistic. We recommend that future research is to develop other metaheuristic approaches or an SA algorithm integrated with other hybrid schemes [27] to improve the computational performance. Parametric analysis of the proposed approach should also be performed.

ACKNOWLEDGMENT

The authors would like to thank Y.-L. Lin for improving the quality of this paper.

REFERENCES

- [1] I. Akyildiz, X. Wang, and W. Wang, "Wireless mesh networks: A survey," *Comput. Netw.*, vol. 47, no. 4, pp. 445–487, Mar. 2005.
- [2] K. Papadaki and V. Friderikos, "Approximate dynamic programming for link scheduling in wireless mesh networks," *Comput. Oper. Res.*, vol. 35, no. 12, pp. 3848–3859, Dec. 2008.
- [3] K. Gokbayrak and E. A. Yildirim, "Joint gateway selection transmission slot assignment, routing and power control for wireless mesh networks," *Comput. Oper. Res.*, vol. 40, no. 7, pp. 1671–1679, Jul. 2013.
- [4] B. Aoun, G. Kenward, R. Boutaba, and Y. Iraqi, "Gateway placement optimization in wireless mesh networks with QoS constraints," *IEEE J. Sel. Areas Commun.*, vol. 24, no. 11, pp. 2127–2136, Nov. 2006.
- [5] J. Crichigno, M.-Y. Wu, and W. Shu, "Protocols and architectures for channel assignment in wireless mesh networks," *Ad Hoc Netw.*, vol. 6, no. 7, pp. 1051–1077, Sep. 2008.
- [6] J. Current, M. Daskin, and D. Schilling, *Discrete network location models*. Berlin, Germany: Springer-Verlag, 2001, ser. Facility Location: Applications and Theory, ch. 3.
- [7] V. Ramamurthi, A. Reaz, D. Ghosal, S. Dixit, and B. Mukherjee, "Channel, capacity, flow assignment in wireless mesh networks," *Comput. Netw.*, vol. 55, no. 9, pp. 2241–2258, Jun. 2011.
- [8] O. E. Muogilim, K.-K. Loo, and R. Comley, "Wireless mesh network security: A traffic engineering management approach," *J. Netw. Comput. Appl.*, vol. 34, no. 2, pp. 478–491, Mar. 2011.
- [9] M. Tang, "Gateways placement in backbone wireless mesh networks," *Int. J. Commun. Netw. Syst. Sci.*, vol. 2, no. 1, pp. 44–50, Feb. 2009.
- [10] A. Franklin and C. S. R. Murthy, "Node placement algorithm for deployment of two-tier wireless mesh networks," in *Proc. 50th Annu. IEEE GLOBECOM*, 2007, pp. 4823–4827.

- [11] A. Hafid, D. Benyamina, and M. Gendreau, "Wireless mesh network planning: A multi-objective optimization approach," in *Proc. 5th Int. Conf. BROADNETS*, 2008, pp. 602–609.
- [12] C. Sánchez, F. Xhafa, and L. Barolli, "Locals search algorithms for efficient router nodes placement in wireless mesh networks," in *Proc. Int. Conf. NBIS*, 2009, pp. 572–579.
- [13] F. Xhafa, A. Barolli, C. Sánchez, and L. Barolli, "A simulated annealing algorithm for router nodes placement problem in wireless mesh networks," *Simul. Model. Practice Theory*, vol. 19, no. 10, pp. 2276–2284, Nov. 2011.
- [14] F. Xhafa, C. Sánchez, and L. Barolli, "Genetic algorithms for efficient placement of router nodes in wireless mesh networks," in *Proc. 24th IEEE Int. Conf. AINA*, 2010, pp. 465–472.
- [15] A. Barolli, C. Sánchez, F. Xhafa, and M. Takizawa, "A tabu search algorithm for efficient node placement in wireless mesh networks," in *Proc. 3rd Int. Conf. INCoS*, 2011, pp. 53–59.
- [16] C.-C. Lin, "Dynamic router node placement in wireless mesh networks: A PSO approach with constriction coefficient and its convergence analysis," *Inf. Sci.*, vol. 232, pp. 294–308, May 2013.
- [17] M. Garey and D. Johnson, *Computers and Intractability - A Guide to the Theory of NP-Completeness*. San Francisco, CA, USA: Freeman, 1979.
- [18] L. Rabiner, "Combinatorial optimization: Algorithms and complexity," *IEEE Trans. Acoust., Speech Signal Process.*, vol. 32, no. 6, pp. 1258–1259, Dec. 1984.
- [19] J. Wang, B. Xie, K. Cai, and D. Agrawal, "Efficient mesh router placement in wireless mesh networks," in *Proc. IEEE Int. Conf. MASS*, 2007, pp. 1–9.
- [20] M. M. Keikha, "Improved simulated annealing using momentum terms," in *Proc. 2nd Int. Conf. ISMS*, 2011, pp. 44–48.
- [21] F. Gonzalez-Longatt, P. Wall, P. Regulski, and V. V. Terzija, "Optimal electric network design for a large offshore wind farm based on a modified genetic algorithm approach," *IEEE Syst. J.*, vol. 6, no. 1, pp. 164–172, Mar. 2012.
- [22] W. H. Ip, D. Wang, and V. Cho, "Aircraft ground service scheduling problems and their genetic algorithm with hybrid assignment and sequence encoding scheme," *IEEE Syst. J.*, vol. 7, no. 4, pp. 649–657, Dec. 2013.
- [23] S. Saha, "GARO framework: A genetic algorithm based resource optimization for organizational efficiency," *IEEE Syst. J.*, vol. 7, no. 4, pp. 889–895, Dec. 2013.
- [24] C.-C. Lin, Y.-Y. Lee, and H.-C. Yen, "Mental map preserving graph drawing using simulated annealing," *Inf. Sci.*, vol. 181, no. 19, pp. 4253–4272, Oct. 2011.
- [25] J. Chen and W. Z. M. Ali, "A hybrid simulated annealing algorithm for nonslicing VLSI floorplanning," *IEEE Trans. Syst., Man, Cybern. C, Appl. Rev.*, vol. 41, no. 4, pp. 544–553, Jul. 2013.
- [26] J. Trovao, V. Santos, P. Pereirinha, H. Jorge, and C. Antunes, "A simulated annealing approach for optimal power source management in a small EV," *IEEE Trans. Sustain. Energy*, vol. 4, no. 4, pp. 867–876, Oct. 2013.
- [27] F. J. Rodriguez, C. Garcia-Martinez, and M. Lozano, "Hybrid metaheuristics based on evolutionary algorithms and simulated annealing: Taxonomy, comparison, synergy test," *IEEE Trans. Evol. Comput.*, vol. 16, no. 6, pp. 787–800, Dec. 2012.



Chun-Cheng Lin (S'06–M'08) received the B.S. degree in mathematics, the Master's degree in business administration, and the Ph.D. degree in electrical engineering from National Taiwan University, Taipei, Taiwan, in 2000, 2007, and 2009, respectively.

From 2009 to 2010, he was an Assistant Professor with National Kaohsiung University of Applied Sciences, Kaohsiung, Taiwan, and from 2010 to 2011, with Taipei Municipal University of Education, Taipei, Taiwan. In February 2011, he joined the National Chiao Tung University, Hsinchu, Taiwan, as an Assistant Professor. Since August 2013, he has been an Associate Professor with the same university. His main research interests include graph drawing and information visualization, wireless networks, design and analysis of algorithms and metaheuristics, and computational management science.



Lei Shu (M'07) received the B.Sc. degree in computer science from South Central University for Nationalities, Wuhan, China, in 2002; the M.Sc. degree in computer engineering from Kyung Hee University, Seoul, Korea, in 2005; and the Ph.D. degree in computer engineering from the National University of Ireland, Galway, Ireland, in 2010.

He was a Specially Assigned Research Fellow with the Department of Multimedia Engineering, Graduate School of Information Science and Technology, Osaka University, Osaka, Japan. He is currently a Full Professor with the College of Electronic Information and Computer, and the Vice Director of the Guangdong Petrochemical Equipment Fault Diagnosis Key Laboratory, Guangdong University of Petrochemical Technology, Maoming, China. His research interests include wireless sensor networks, sensor network middleware, multimedia communications, and security.

Dr. Shu is a member of the Association for Computing Machinery and the European Alliance for Innovation.



Der-Jiunn Deng (M'00) received the Ph.D. degree in electrical engineering from the National Taiwan University, Taipei, Taiwan, in 2005.

In August 2005, he joined the Department of Computer Science and Information Engineering, National Changhua University of Education, Changhua, Taiwan, as an Assistant Professor. Since February 2012, he has been a Full Professor with the same university. His research interests include multimedia communications, quality of service, and wireless networks.

Dr. Deng served or is serving on several symposium chairs and technical program committees for IEEE and other international conferences. He also served or is serving as an Editor and as a Guest Editor for several technical journals. He received the Top Research Award of National Changhua University of Education in 2010.